Multi-Walled Carbon Nanotube-Gold Nanocomposites toward Oxygen Reduction Reaction

Keqiang Ding[1,], Hongwei Yang[1], Yanli Cao[1], Chunbao Zheng [1], Lu Liu[1], Likun Liu[1], Yiran Wang[2], Xingru Yan[2], and Zhanhu Guo[2,*]*

[1] College of Chemistry and Materials Science, Hebei Normal University, Shijiazhuang 050024, P.R. China
[2] Integrated Composites Laboratory (ICL), Dan F. Smith Department of Chemical Engineering, Lamar University, Beaumont, TX 77710, USA
[*]E-mail: dkeqiang@263.net; zhanhu.guo@lamar.edu

Multi-walled carbon nanotubes (MWCNTs) nanocomposites decorated with Au nanoparticles were prepared by the facile pyrolysis of $AuCl_3$ dissolved in room temperature ionic liquids (RTILs) of 1-ethyl-3-methylimidazolium tetrafluoroborate (EMIBF4) in the presence of MWCNTs. X-ray diffraction (XRD) and scanning electron microscopy (SEM) were used to characterize the obtained samples. The results showed that highly crystalline Au particles with an average diameter of 300 nm were fabricated. The electrocatalytic performance of the Au particles modified glassy carbon electrode in the oxygen reduction reaction (ORR) was probed using cyclic voltammetry (CV). The pyrolysis time was noticed to be a key factor, influencing not only the size of Au particles but also the electrocatalytic activity of Au particles towards ORR. It revealed that under the same conditons the Au particles with a diameter close to 300 nm showed the largest current of ORR among the prepared samples.

1. INTRODUCTION

Recently, the development of low temperature fuel cells, including proton exchange membrane fuel cells (PEMFC), direct methanol fuel cells (DMFC), direct ethanol fuel cells (DEFC), has been intensively pursued due to their unique properties, such as their higher energy-conversion efficiency, providing high-energy output with no harmful by-products compared to the traditional batteries [1,2]. In the fuel cells, oxygen reduction reaction (ORR) is the only employed cathodic reaction to receive

electrons released from methanol, ethanol or other small organic molecules [3]. Hence, catalysts used for the ORR have been widely investigated [4, 5]. Among the developed catalysts used for ORR, the metal of gold is regarded as a main catalyst due to its chemical stability, specific optical and other physical properties [6]. For example, El-Deab et al. have studied ORR on an Au nanoparticles modified carbon electrode, and pointed out that the electrocatalytic activity of the Au nanoparticle-based electrodes is inherently related to its electrodeposition conditions (i.e., the absence or presence of some additives) as well as the nature of the substrate [7]. Rezwan Miah et al. investigated ORR [8] at a Sn-adatoms-modified Au (poly) electrode by the hydrodynamic voltammetric technique, and demonstrated that the underpotential deposited Sn-adatoms on the Au (poly) electrode substantially promoted the activity of the electrode towards an exclusive one-step four-electron ORR. Kumar et al. [9] have studied ORR on a carbon-supported unalloyed Au–Pt bimetallic nanoparticles prepared by using a polyol method, and addressed that the half-wave potential for ORR on bimetallic Au–Pt/C is ~100mV less negative when compared with that of Pt/C. To our knowledge, there are no papers reporting ORR occurring at an Au particles with a diameter more than 300 nm modified electrode.

Currently, two typical methods are reported to synthesize Au nanoparticles. (i) Chemical reduction reaction. For example, Terzi et al. [10] addressed the Au/Pt bimetallic nanoparticle systems, in which $NaAuCl_4 \cdot 2H_2O$ and $NaBH_4$ were employed as the Au precursor and the reductive reagent, respectively. Stoyanova et al. [11] described the preparation of Au nanoparticles, where $HAuCl_4$ and sodium citrate were used as the starting materials. (ii) Electrochemical reduction reaction. For instance, Zhang et al. [12] immobilized Au nanoparticles on the as-grown and oxygen-terminated (O-terminated) boron-doped diamond (BDD) films electrochemically, in which the deposition solution was 0.1M H_2SO_4 containing 0.3 mM of $AuCl_4^-$ solution. Meanwhile, CNTs have attracted a great deal of attention owing to their exceptional mechanical, electronic and chemical properties [13, 14], and have served as an ideal substrate to modify the electrode surface [15]. Thus, immobilizing metal nanoparticles on CNTs has turned into an interesting field mainly due to the key roles of CNTs and metal nanoparticles in the field of electrocatalysis, biosensors and so on [16]. To the best of our knowledge, no paper reporting the immobilization of Au particles, prepared by a pyrolysis method using RTILs as the solvent, on the CNTs was published.

Due to its excellent features, for instance, low-volatility, non-toxicity, non-flame, higher conductivity compared to common organic solvent, and higher solubility for organic substance when comparing with aqueous solution, room temperature ionic liquids (RTILs) have attracted much more attention [17]. RTILs are mainly applied in the following fields of chemistry, (1) being used as solvents in organic synthesis [18]. (2) Being employed as electrolytes in electrochemistry [19]. However, to our knowledge, except for our previous work [20], the application of RTILs in pyrolysis process was rarely reported so far.

In this paper, multi-walled carbon nanotubes (MWCNTs) nanocomposites decorated with highly crystalline Au particles were prepared through a very simple hydrolysis method using ionic liquid of 1-ethyl-3-methylimidazolium tetrafluoroborate (EMIBF4) as the solvent, in which no other reducing reagents were introduced. X-ray diffraction (XRD), scanning electron microscopy (SEM) and energy dispersive spectroscopy (EDS) were employed to characterize the samples obtained. The

electrocatalytic activities of Au particles towards ORR were evaluated by cyclic voltammetry (CV) in a 0.1 M Na_2SO_4 solution.

2. EXPERIMENTAL

2.1 Reagents and Materials

MWCNTs (purity>95%) of 10-20 nm diameter were purchased from Shenzhen nanotech port Co., Ltd. (China). Room temperature ionic liquid of 1-ethyl-3-methylimidazolium tetrafluoroborate (EMIBF4) with a purity of more than 99% was obtained from Hangzhou Chemer Chemical Co., Ltd. (China). All the electrodes were bought from Tianjin Aida Co., Ltd (China). All other chemicals were analytical grade and were used without further purification. Deionized water was used to prepare the aqueous solutions.

2.2 Preparation of MWCNT-Au Nanocomposites

MWCNTs-Au nanocomposites were synthesized by a simple pyrolysis process. Briefly, 4 mL 5×10^{-3} M $AuCl_3 \cdot HCl \cdot 4H_2O$ (using EMIBF4 as the solvent) and 10 mg MWCNTs were mixed to yield a suspension solution, whcih was then ultrasonicated for 30 min. The suspension was then placed in a home-made autoclave at room temperature, and then the well-sealed autoclave was transferred to a box-type furnace. The temperature of the box-type furnace was increased to 200 ℃ within 30 min, and then it was maintained at this temperature for a certain period to complete the pyrolysis process. The filtered samples were thoroughly washed with redistilled water, and then dried in ambient conditions to generate the Au particles that were supported by MWCNTs (denoted as MWCNTs-Au).

2.3 Preparation of MWCNTs-Au Modified Electrode

Prior to each experiment, the working electrode of a glassy carbon (GC) electrode with a diameter of 2 mm was successively polished with 1 and 0.06 μm alumina powders on a piece of microcloth wetted with doubly distilled water, which gave an electrode with a mirror-like surface. For the preparation of MWCNTs-Au coated electrode, 3.0 mg of the resultant material was added to a 1 mL ethanol solution of Nafion (the content of Nafion being 0.5 wt.%), and then the mixture was treated for 30 min with ultrasonication to form a uniform suspension. The obtained suspension (5 μL) was dropped onto the surface of a well-treated GC electrode. Finally, the resultant MWCNTs-Au modified GC electrode was dried with hot air.

2.4 Characterization

XRD analysis of the catalyst was carried out on a Bruker D8 ADVANCE X-ray diffractometer equipped with a Cu Kα source (λ= 0.154 nm) at 40 kV and 30 mA. The 2θ angular region between 10

and 80° was explored at a scan rate of 1°/step. The samples obtained were characterized using SEM (S-4800, HITACHI, Japan). Energy dispersive spectroscopy (EDS) spectrum analysis was carried out on an X-ray energy instrument (EDAX, PV-9900, USA). The pyrolysis process was implemented in a SRJX-8-13 box-type furnace equipped with a KSY 12-16 furnace temperature controller.

Electrochemical experiments were conducted on a model CHI660B electrochemical workstation (Chen-hua, Shanghai, China). A conventional three-electrode system was employed, in which a MWCNTs-Au modified GC electrode and platinum wire were used as the working electrode and counter electrode, respectively. It should be noted that the reference electrode was a saturated calomel electrode (SCE). All potentials in this paper are reported with respect to SCE. Electrochemical impedance spectroscopy (EIS) is performed in the frequency range from 1 to 10^5 Hz with an applied amplitude of 5 mV at the open circuit potential (OCP). Prior to the ORR experiment, the electrolyte of 0.1 M Na_2SO_4 was purged by nitrogen for 20 min, and then it was bubbled by oxygen gas for 30 min to form an oxygen-saturated 0.1 M Na_2SO_4, as described in our previous work [21]. All the experiments are carried out at room temperature.

3. RESULTS AND DISCUSSION

3.1 XRD Analysis

Fig.1A shows the typical XRD patterns of the samples. For pattern (**a**) in Fig. 1A, the diffraction peak at 26.1° was indexed to the (002) plane of CNTs (JCPDS card: 26-1077), which is consistent with the previous report [22]. After 3-hour pyrolysis, the diffraction peak corresponding to MWCNTs was still clearly observed, suggesting that the pyrolysis process did not destroy the crystal structure of the MWCNTs. Meanwhile, some new peaks located at 38, 45, 65 and 78° were displayed, as shown in pattern b, which correspond to the (111), (200), (220) and (311) planes of the single face-centered cubic (fcc) structure of gold (00-004-0784), respectively [23]. Since no other diffraction peaks were noticed, Fig. 1A, it strongly demonstrates that only Au particles were formed on the surface of the MWCNTs. The average crystallite size (*t*) was estimated by using the Debye-Scherer formula, $t=0.89\lambda/(\beta \cdot \cos\theta_B)$ [24], where λ is the X-ray wavelength (1.54 Å), θ_B is the Bragg diffraction angle, and β is the peak width at half-maximum. Based on this formula, the average crystallite sizes of Au particles was estimated to be 8.3 nm from the (111) peak, which was rather smaller than that observed in SEM images, image d in Fig.2B, indicating that the particles are polycrystalline structure.

Fig.1B shows the EDS spectra of the obtained samples. As shown by curve a, for the pure MWCNTs, except for small amount of Al and Fe (from MWCNTs themselves during the preparation), the main peak corresponding to the element C is displayed. While for the obtained samples prepared by 3-hour pyrolysis, some novel peaks corresponding to the element of Au were clearly displayed, indicating that Au was fabricated during the pyrolysis process, which is consistent with the XRD spectra shown by pattern b in Fig.1A very well, namely, only pure Au particles were produced by the developed pyrolysis method. The weight percent of the precursors containing MWCNTs before pyrolysis for C, Al, Fe and Au are 86.4, 1.0, 2.3 and 1.9 wt%, respectively.
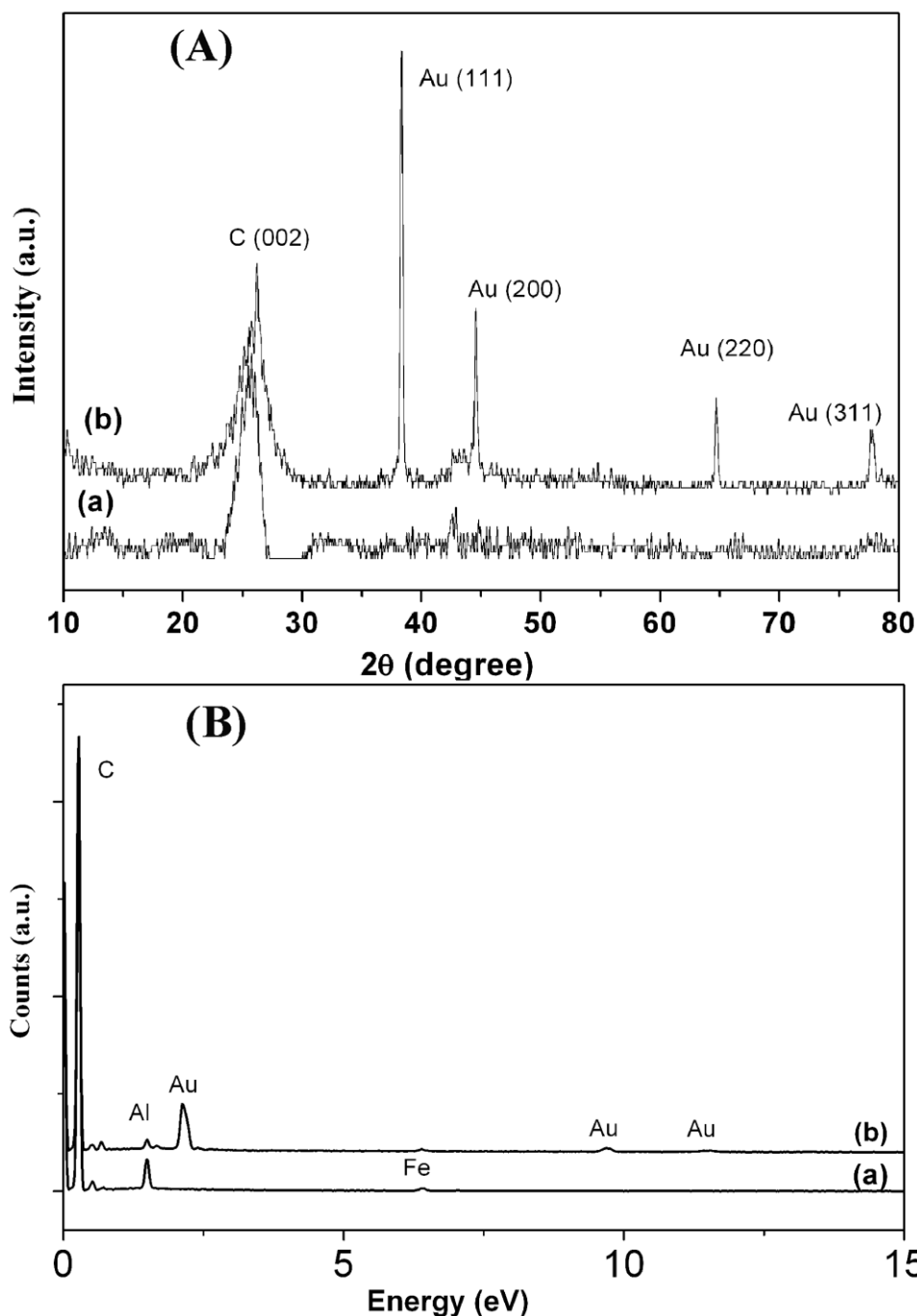
Figure 1. **(A)**. XRD patterns of pure MWCNTs (a), and MWCNT-Au samples after pyrolysis for 3 hours (b); and **(B)**. EDS spectra for pure MWCNTs (a), and for MWCNT-Au samples after pyrolysis for 3 hours (b).

After 3-hour pyrolysis, the weight percent of the sample for C, Al, Fe and Au are 82.0, 0.5, 0.5 and 10.0 wt%, respectively. It confirmed that the samples were Au particles coated MWCNTs rather than MWCNTs coated Au particles (since the amount of C is larger than that of Au after treatment). In addition, one can see that after pyrolysis process, the content of Au was significantly increased, and the content of C, Al and Fe was lowered evidently.
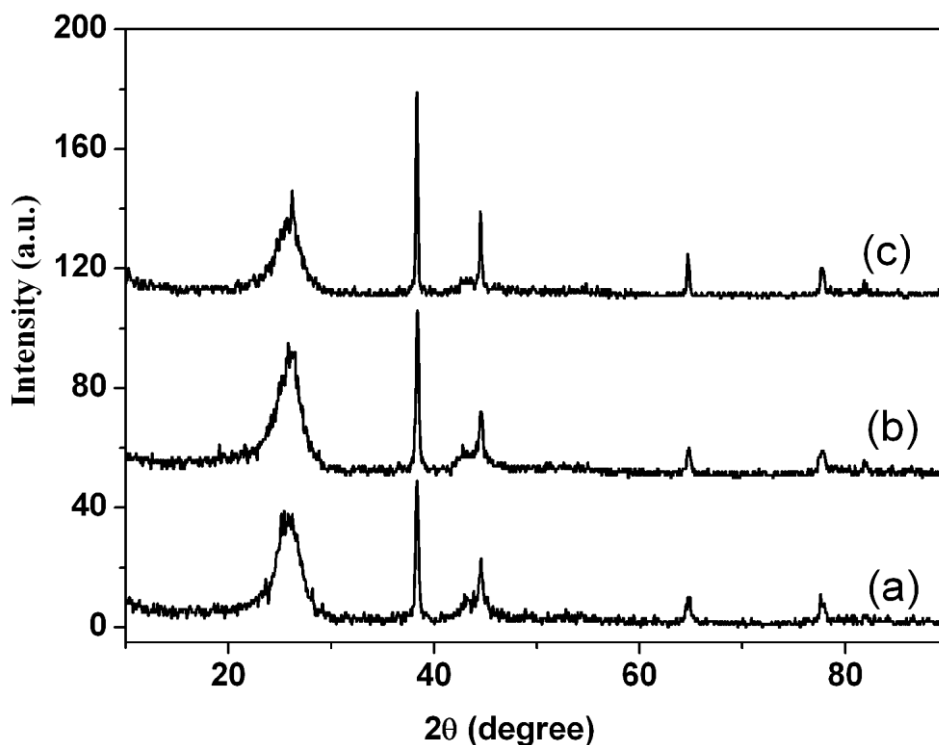
Figure 2. XRD patterns of the samples prepared by pyrolysis for different periods. Pattern (**a**): 1 h; (**b**): 2 h; and (**c**): 3 h.

The pyrolysis time is a key parameter that can affect the resultant sample in both the size and the crystal structure. Thus, the influence of pyrolysis time on the resultant samples was probed. As shown by Fig.2, the XRD patterns of the resultant samples varied greatly with the employed pyrolysis time. It can be seen that the intensities of diffraction peaks, corresponding to the planes of (111), (200), (220) and (311) of the sample prepared by 3-hour pyrolysis (as shown by pattern c) are higher than those for the sample produced for 1-hour pyrolysis (as shown by pattern a). It indicated that the crystallinity of the sample obtained by pyrolysis of 3-hour is better than that fabricated by 1-hour pyrolysis [25]. Additionally, the intensity of the diffraction peak corresponding to carbon (002) for the sample prepared by 3h, is somewhat lowered compared to the sample prepared by 1-hour pyrolysis (as shown by pattern a). It indicated that the crystal structure of MWCNTs was demolished in some degree.

3.2 SEM Characterization

Fig. 3 shows the SEM microstructures of the samples prepared by pyrolysis for various periods. For the precursor containing $AuCl_3$ and MWCNTs, as shown by (a), a particle with well-defined crystal structure circled by red line was displayed, as proven to be pure Au particle by the localized EDS. Meanwhile, some irregular and layered particles circled by green line were also displayed, as testified to be $AuCl_3$ by the localized EDS measurement. One can see from image b and c that the irregular particles became smaller and smaller with increasing the pyrolysis time, lastly, when the

pyrolysis time reaches 3 hours, to our surprise, the irregular particles vanished and huge particles with well-defined structure and diameter close to 300 nm were prepared.
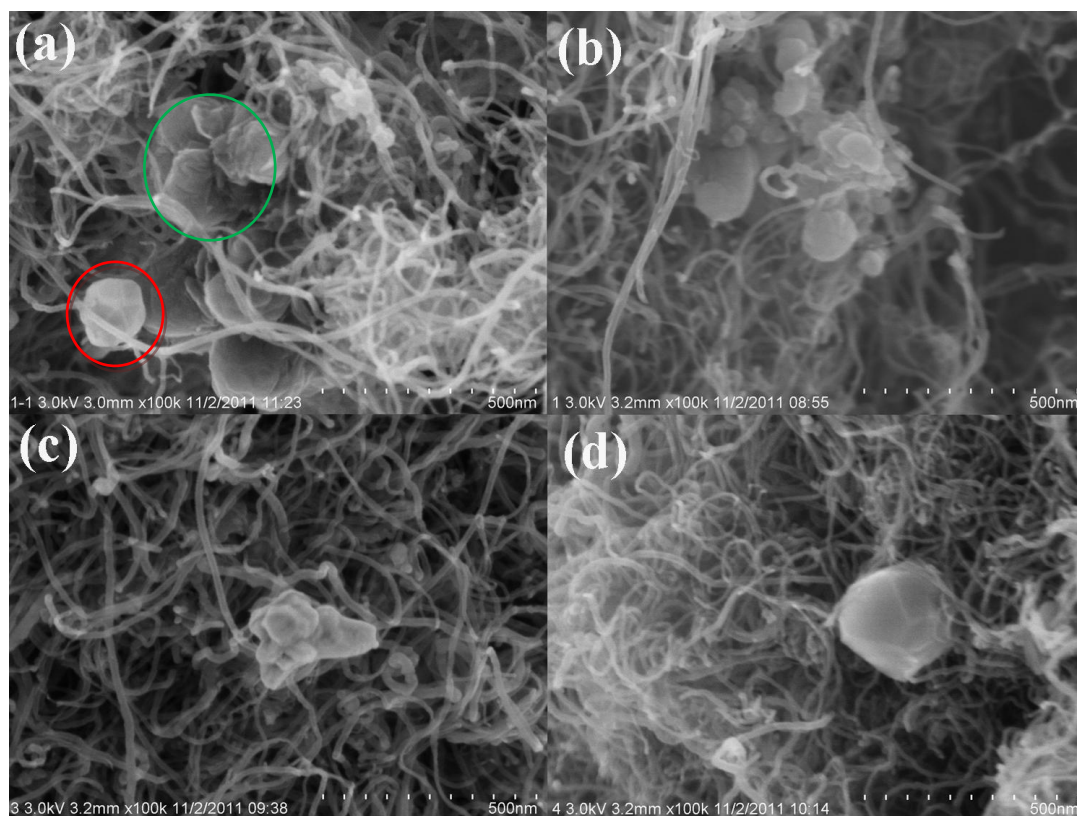

Figure 3. SEM images of the samples prepared by pyrolysis for different time. Image (**a**): precursors containing MWCNTs and AuCl$_3$; image (**b**): 1 h; image (**c**): 2 h; image (**d**): 3 h.

Bao et al. [26] described the preparation of Au nanoparticles, in which HAuCl$_4\cdot$3H$_2$O and NaBH$_4$ were employed as the gold precursor and reducing reagent, respectively. Zhan et al. [27] reported the synthesis of Au nanoparticles, using Cacumen Platycladi (CP) leaf as the reducing agent. Thus, there must be a reductive reagent to reduce Au^{3+} to yield Au atoms, leading to the formation of Au particles. What is the reductive reagent in the above pyrolysis process and how to explain the pyrolysis process? Numerous attempts justified that Au particles could not be fabricated by this pyrolysis process in the absence of MWCNTs. Thus, the MWCNTs were employed as the main reducing reagents in the above pyrolysis process while Al was used as the reducing reagent in the mixing process prior to pyrolysis.

Fig.4 depicts the digital photos of the solutions used in the pyrolysis process. A red-yellow solution was produced as shown by image b when AuCl$_3$ was dissolved in EMIBF4. While, after pyrolysis process in the absence of MWCNTs, a thick red-yellow solution was presented, as shown by image c. The color change strongly indicated that some reactions happened between AuCl$_3$ and EMIBF4. However, under this condition, it was found that Au particles could not be prepared. In the presence of MWCNTs after pyrolysis for 3 hours, the filtered solution became colorless, as shown by

image d. It indicated that Au^{3+} was totally consumed by this pyrolysis process. That is to say, MWCNTs were used as a reducing reagent in the pyrolysis process.
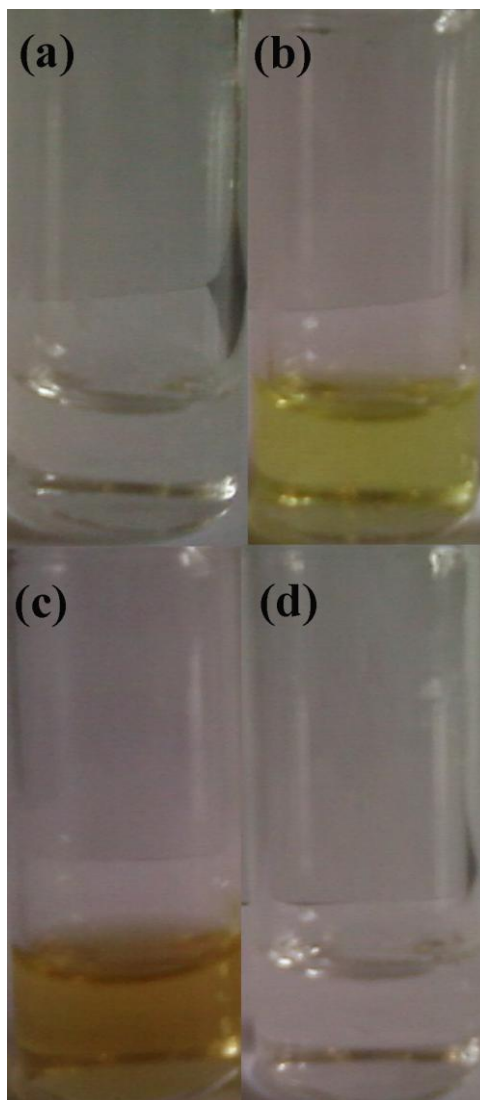

Figure 4. Digital photos for the solutions. Photos (**a**): Pure EMIBF4; (**b**): EMIBF4 containing AuCl₃; (**c**): EMIBF4 containing AuCl₃ in the absence of MWCNTs; and (**d**): The filtered solution in the presence of MWCNTs.

Fig.5 shows the ultraviolet-visible (UV-vis) absorption spectra for the solution appearing in the pyrolysis process. As shown by curve a, no evident peak can be observed for the pure RTILs of EMIBF4 [28]. Also, except for a small absorption peak at around 250 nm, no obvious change can be found in curve b, indicating that there is a weak interaction between Au^{3+} and EMIBF4. To our surprise, for the colorless solution, corresponding to photo d in Fig. 4, an absorption peak at around 290 nm was observed as shown by curve Figure 5(c). Bao et al. [26] investigated the UV-vis spectra of Au^{3+} aqueous solution, and thought that the shoulder peak at around 290 nm could be assigned to the ligand-to-metal charge-transition, indicative of the formation of complexes. Thus, it can be

confirmed that some new complexes were prepared after the pyrolysis process based on the UV-vis spectra shown in Fig.5.
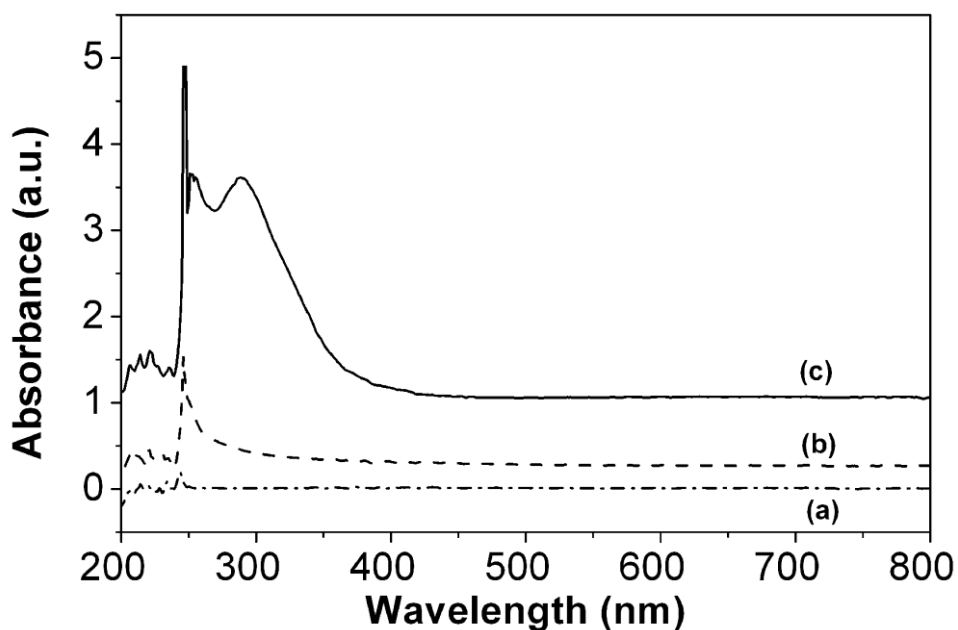

Figure 5. UV-Vis spectra for samples. Curve **a**: Pure ionic liquids of EMIBF4; curve **b**: EMIBF4 containing $AuCl_3 \cdot HCl \cdot 4H_2O$ after pyrolysis in the absence of MWCNTs; curve **c**: The filtered EMIBF4 after pyrolysis in the presence of MWCNTs.

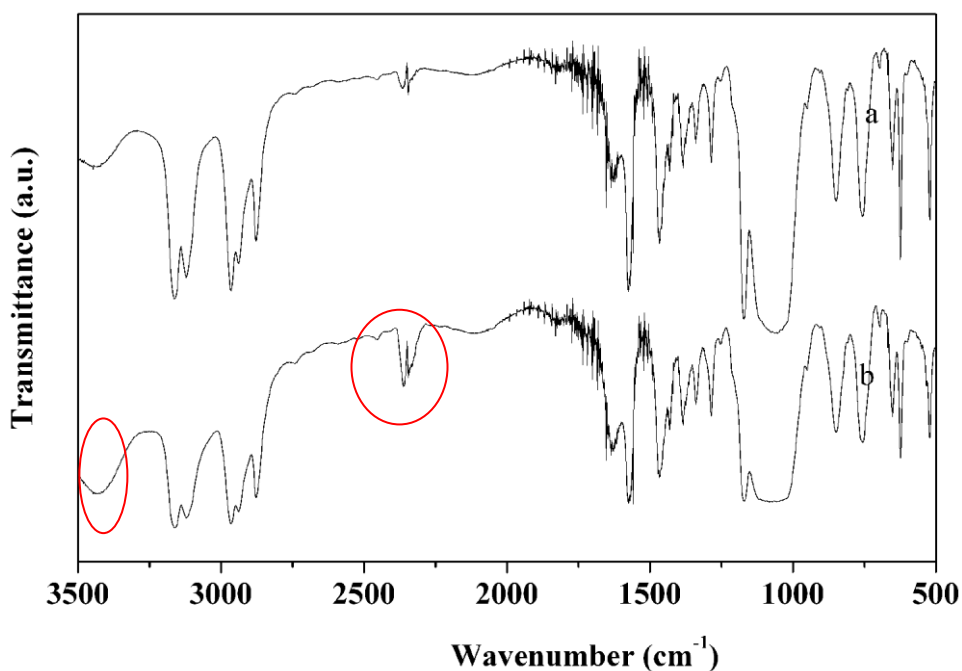**Figure 6**. FT-IR spectra for the $EMIBF_4$ containing $AuCl_3 \cdot HCl \cdot 4H_2O$ and CNTs. Cure **a** and **b** correspond to sample before and after pyrolysis, respectively.

Fig.6 shows the FT-IR spectra of the samples before and after pyrolysis, in which MWCNTs were filtered prior to the measurement. Based on the previously published work [29], the bands at 767 and 858 cm^{-1} are assigned to the stretching vibration of BF_4^-, and C-H in-plane vibration of imidazolium ring, respectively. And the band at 1576 cm^{-1} corresponds to the in-plane C-N stretching vibrations of the imidazolium ring. One can see that after 3-hour pyrolysis, the intensities of all the absorption peaks were greatly attenuated compared with those of the starting materials as shown by curve a. It indicates that some groups in EMIBF4 have reacted with the introduced Au^{3+} and MWCNTs since the band intensity of FT-IR spectra is proportional to the amount of EMIBF4[30]. Interestingly, as shown by the red-circled parts, two evident absorption peaks, at around 2350 and 3410 cm^{-1} are displayed clearly, indicative of the formation of **more amount** of groups. FT-IR spectra strongly demonstrated that some reactions took place between the EMIBF4 and the introduced Au^{3+} or MWCNTs.

Generally, due to the self-oxidation, the surface of MWCNTs is decorated with oxygen-containing functional groups, from compounds such as carboxylic acids, phenols, lactones, carboxylic anhydrates, ketones, ethers, quinones or pyrones [31]. Therefore, in such a sealed autoclave, i.e., at the temperature of 200 °C and under a higher pressure, Au^{3+} can be easily reduced to yield Au atoms by some organic groups that are attached to the surface of the MWCNTs, for instance, CNTs-COOH $+Au^{3+} \rightarrow CNTs + Au^0 + H^+ + CO_2 \uparrow$ [32] .

Close inspection revealed that after ultrasonication, some nanoparticles with a diameter of around 150 nm and well-defined crystal structure were observed in the mixture containing $AuCl_3$ and MWCNTs, as shown by the red-circled part in image a of Fig.3. The localized EDS spectra indicated that these nanoparticles have only element of Au, and these layered particles circled by green line in image a have only two elements, i.e., Cl and Au (data no shown here). That is to say, the small regular particles circled by red line in image a of Fig. 3 are Au particles, and the irregular layered particles are the starting materials of $AuCl_3$ rather than other substances. How are these Au nanoparticles formed? As shown by the circled part in curve a in Fig.1(B), EDS spectra revealed that small amount of Al, which came from the preparing process of CNTs[33], were maintained in MWCNTs, thus, under the ultrasonication condition, the residue Al can react with $AuCl_3$ to generate Au atoms by a chemical reaction. As a result, some particles of Au with a smaller diameter were fabricated in the precursor containing $AuCl_3$ and MWCNTs.

What is the formation process of the Au particles with a diameter close to 300 nm? It is reported that low charges and asymmetrically distributed charges are the key factors causing nanoparticle aggregation [34]. EMIBF4, which has a lower dielectric constant [35] compared to water, can decrease the surface charge of the formerly existed Au nanoparticles due to the change in polarity of the solvent. Therefore, similar to the case described by Wang et al. [36], the newly formed Au atoms, prepared by a reduction reaction by MWCNTs, can migrate from the solution of EMIBF4 to the EMIBF4/Au (formerly prepared by a chemical reaction between Al and Au^{3+} as stated above.) interface in sequence, which is also analogous to the nanoparticle self-assembly at the toluene/water or hexane/water interface in ethanol-mediated methanol [37, 38]. As a result, Au particles with a diameter more than 300 nm were generated.

3.3 Electrocatalysis of Au particles towards oxygen reduction reaction (ORR)
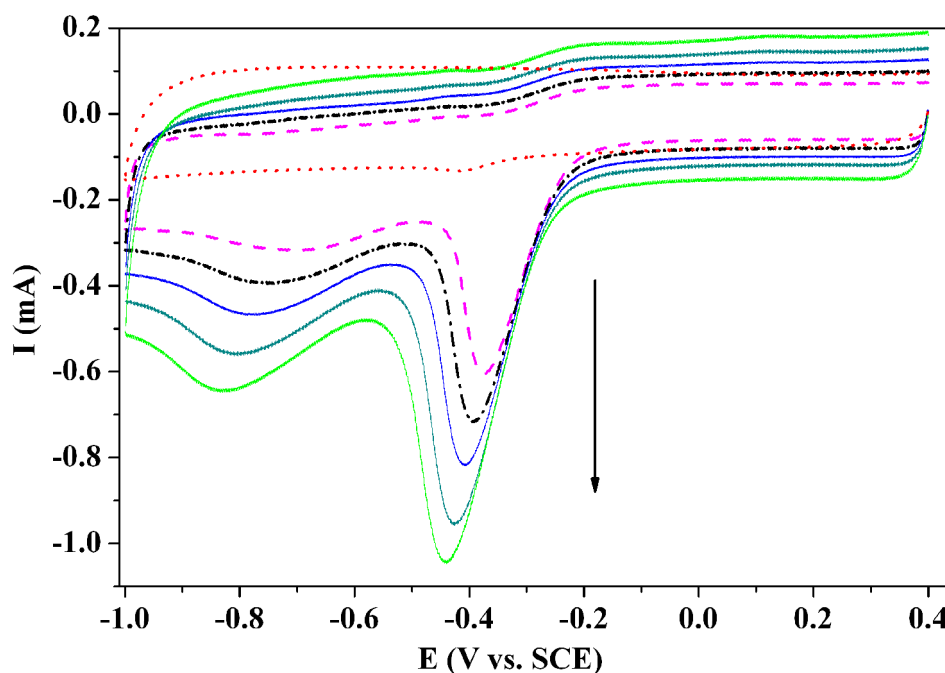

Figure 7. CVs obtained on a MWCNTs-Au coated GC electrode in 0.1 M Na_2SO_4 aqueous solution. The dotted red line was measured in a nitrogen gas saturated 0.1 M Na_2SO_4 at scan rate of 80 mV/s, while other lines were conducted in an oxygen gas saturated 0.1 M Na_2SO_4, scan rates as shown by the arrow are 60, 80, 100, 120 and 150 mV/s, respectively.

Due to the key role of ORR in fuel cells, many works on ORR have been widely investigated [39]. As addressed above, the electrodes decorated with nanoparticles, on which ORR can undergo, have been intensively studied. To the best of our knowledge, the ORR occurring on Au particles, which were prepared by pyrolysis using RTILs as the solvents, has not been reported.

Fig. 7 shows the cyclic voltammograms (CVs) of ORR in 0.1 M Na_2SO_4 aqueous solution on the MWCNTs-Au modified GC electrode. As shown by the red line, in the nitrogen gas saturated solution, no reduction peaks can be observed. While, in the oxygen-saturated solution, a series of CV curves obtained at various scan rates were clearly displayed. The first reduction peak currents at around -0.4 V vs SCE in the negative-direction potential scan are linear to the square root of scan rates (data not shown here), indicating that the process of ORR on the modified electrode was determined by a diffusion-controlled process [40]. Also, it suggested that those reduction peaks were resulted from the introduced oxygen rather than other substances. It is well-known [41] that the first peak appearing at relatively positive potential is assigned to the formation of HO_2^- according to the reaction (1).

$$O_2 + H_2O + 2e = HO_2^- + OH^- \qquad (1)$$
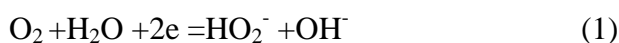
While the second consecutive peak appearing at relatively lower potential at around -0.8 V vs SCE is assigned to the further reduction of the electrogenerated HO_2^- according to the reaction (2) [42].

$$HO_2^- + H_2O + 2e = 3OH^- \qquad (2)$$

CVs of ORR on the MWCNTs modified GC electrode were also plotted in Fig.8. It can be seen that the cathodic peaks, located at around -0.4V (peak 1) and -0.7V(peak 2), measured on the MWCNTs-Au modified GC electrode were greatly positively shifted for about 80 and 120 mV, respectively, when compared to those CVs displayed on the MWCNTs-coated GC electrode. Meanwhile, the cathodic peak currents measured on the MWCNTs-coated GC electrode were significantly increased when compared to that measured on the MWCNTs-Au coated GC electrode, for example, the peak currents corresponding to peak 1 and 2 were enhanced, respectively, from 0.3 to 0.7 mA and from 0.3 to 0.38 mA. That is to say, Au particles have catalyzed the ORR significantly when compared to the case measured on the MWCNTs-modified GC electrode. It strongly proved that the overpotential in ORR was significantly attenuated by the formed Au particles [43].
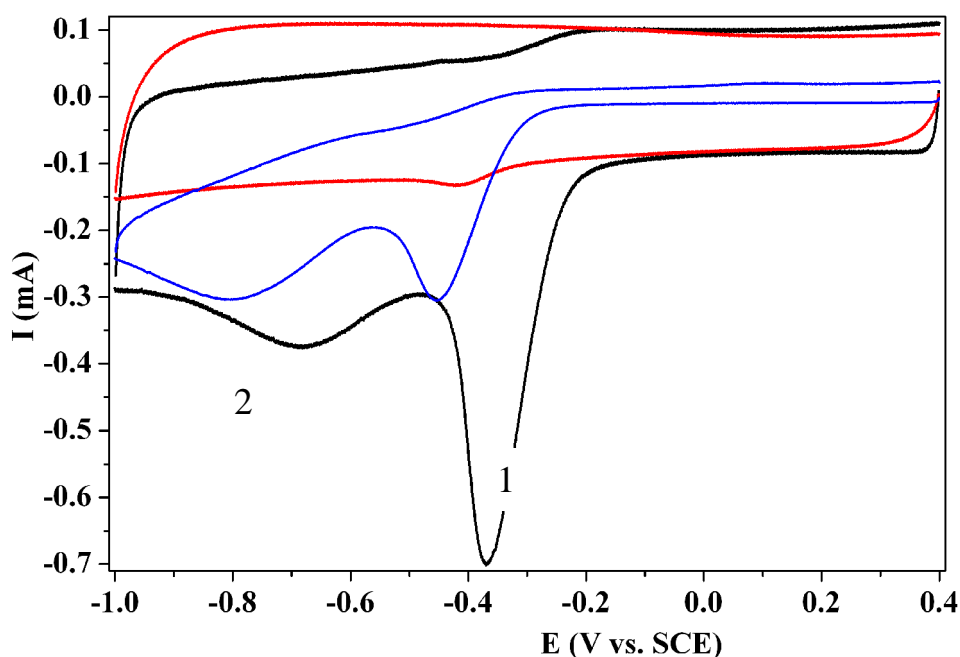

Figure 8. CVs obtained in 0.1 M Na_2SO_4 aqueous solution. Red line was measured on a MWCNTs-Au coated GC electrode in a nitrogen gas saturated 0.1 M Na_2SO_4 aqueous solution; the blue and black lines were recorded on a MWCNTs and MWCNTs-Au coated GC electrode, respectively, in which the electrolyte was an oxygen saturated 0.1 M Na_2SO_4. All scan rates are 80 mV/s.

Evidently, the pyrolysis time employed has a strong influence on the morphology and size of the resultant Au particles, which can greatly affect the electrocatalysis of the as-prepared Au particles towards ORR. Therefore, three kinds of MWCNTs-Au composite catalysts were prepared, in which the pyrolysis time was different from each other. As shown in Fig.9, the reduction peak currents increased with the pyrolysis time employed. Under the same conditions, the largest current was observed on the 3h prepared MWCNTs-Au coated GC electrode. Obviously, with increasing the

pyrolysis time, more Au particles were fabricated, leading to more active surface of Au on which ORR can occur. This result is consistent with the result obtained from SEM images, Fig.3, i.e., more large Au particles were created with the increasing pyrolysis time. Also, one can see that for all the three samples the reduction peak potentials of ORR were slightly different from each other. Probably, it indicated that some unknown synergistic reactions took place between the MWCNTs and the formed Au particles, which can influence the process of ORR [44].
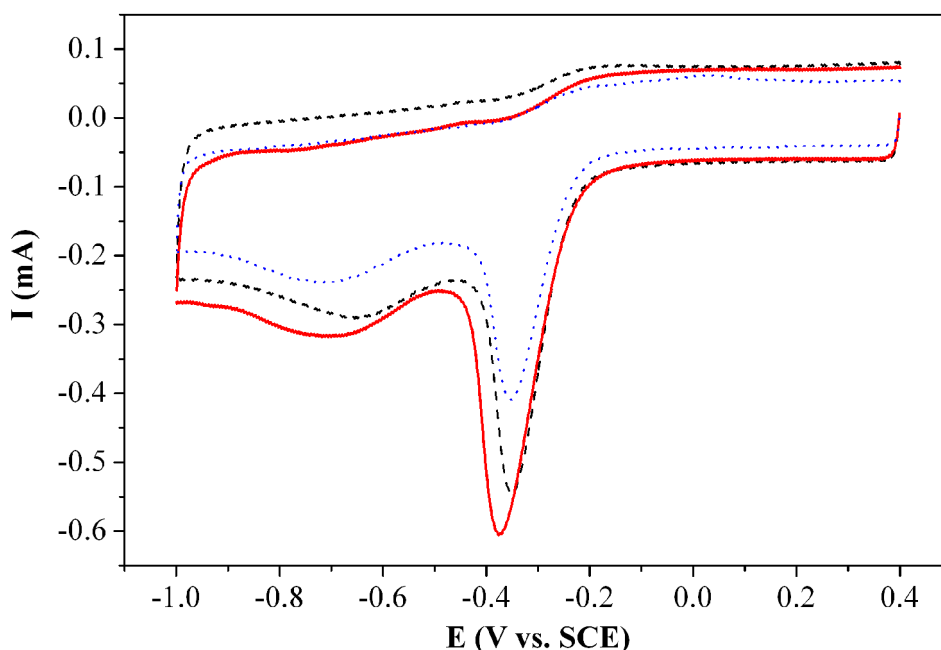

Figure 9. CVs obtained on MWCNTs-Au coated GC electrode in oxygen saturated 0.1 M Na_2SO_4 solution, in which the MWCNTs-Au were prepared by pyrolysis for various periods. Dotted line: 1 h; dashed line: 2 h; solid line: 3 h. Scan rate: 50 mV/s.

Nyquist plot, one type of curves in the Electrochemical Impedance Spectroscopy (EIS), is a main method for evaluating the electrochemical performance of the working electrode [45]. Nyquist plots for the MWCNTs-Au coated GC electrode were conducted as illustrated in Fig.10. Generally, based on the previous reports [46,47], the semicircle appearing at the high frequency region corresponds to a circuit having a resistance element parallel to a capacitance element, and a semicircle with a larger diameter corresponds to a larger charge transfer resistance. Thus, approximately, the diameter of the semicircle stands for the value of charge transfer resistance. One can see from Fig.10 that the diameter of the semicircle appearing in the higher frequency region greatly varied with the pyrolysis time. Curve a, corresponding to the MWCNTs-Au composites that were fabricated by 3-hour pyrolysis, has the smallest semicircle, indicating that the charge transfer resistance of ORR on the 3-hour prepared Au-MWCNTs composite catalyst is the smallest one among the three samples, which is consistent with the results obtained from Fig.9.

Chronoamperometry is a powerful technique to compare the electrocatalysis of various catalysts [48, 49]. The current-time curves were conducted at a potential of -0.35 V versus SCE. It can

be seen from Fig.11 that the steady-state current plateau of curve c, i.e., corresponding to the sample that was prepared by 3-hour pyrolysis, is the highest one among the three samples.
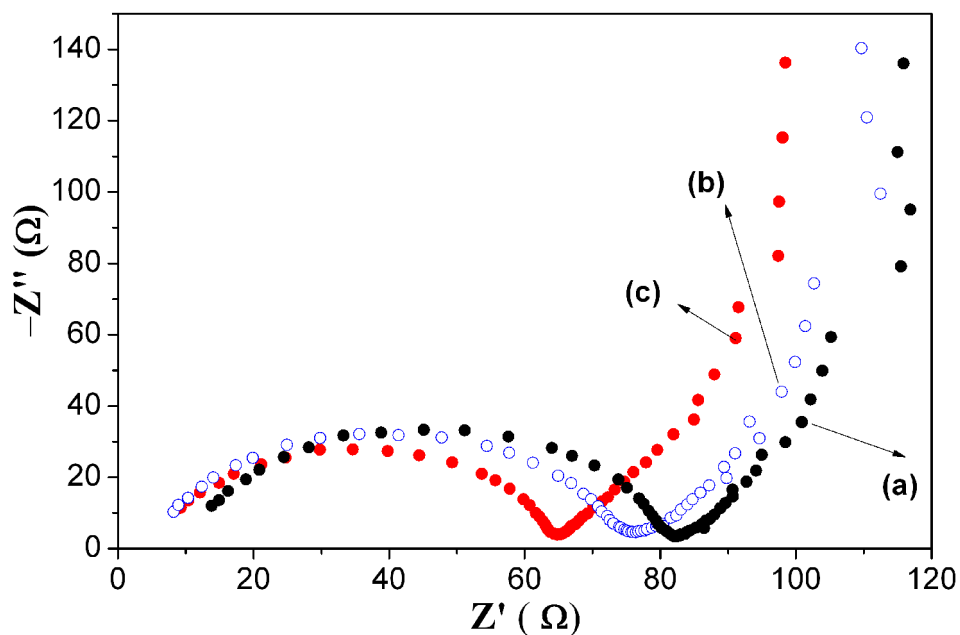

Figure 10. Nyquist plots for the MWCNTs-Au coated GC electrode in the oxygen saturated 0.1 M Na$_2$SO$_4$ solution, in which the MWCNTs-Au nanocomposites were prepared by pyrolysis for various time periods. These curves were measured at the open circuit potential. Line (**a**): 1 h; line (**b**): 2 h; line (**c**): 3 h.
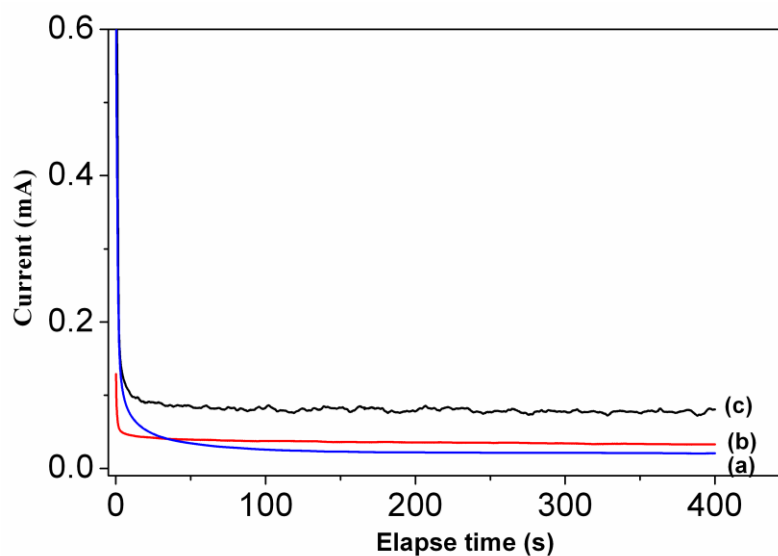

Figure 11. Chronoamperometry curves of MWCNTs-Au coated GC electrode in an oxygen saturated 0.1 M Na$_2$SO$_4$ solution at -0.35 V vs. SCE. The pyrolysis time for line **a**, **b** and **c** are 1, 2 and 3 h, respectively.

For example, at the time of 200 s, the current for curve a, b and c is 0.026, 0.038 and 0.082 mA, respectively. With the increase of the pyrolysis time, more Au particles were generated, leading to more active surface of Au particles towards ORR, thus, the electrocatalysis of the sample corresponding to curve c is superior to those samples prepared by pyrolysis for 1 and 2 hours. This result is consistent with those results obtained in Fig.9 and Fig.10.

4. CONCLUSION

For the first time, highly crystalline Au particles with an average diameter of 300 nm were prepared by a simple method of pyrolysis of $AuCl_3$ dissolved in EMIBF4 ionic liquid in the presence of MWCNTs, in which no other reducing reagents were introduced. XRD, SEM and EDS were all employed to characterize the as-prepared samples, showing that Au particles with a well-defined crystal structure were generated by this novel method. Also, CVs of ORR indicated that the as-prepared Au particles can electrocatalyze the ORR in neutral solution. And further work revealed that the electrocatalysis of the Au particles towards ORR is closely related to the pyrolysis time employed. The main contribution of this work is in demonstrating a one-step pyrolysis reaction using RTILs as the solvents for synthesizing Au particles on MWCNTs, which is expected to be helpful for the preparation of other kinds of metal particles on a large scale.

References

1. S.-E. Jang, H. Kim, *J. Am. Chem. Soc.*, 132(2010)14700.
2. S. Guo, S. Zhang, X. Sun, S. Sun, *J. Am. Chem. Soc.*, 133(2011) 15354.
3. J. L. Fernández, V. Raghuveer, A. Manthiram, A. J. Bard, *J. Am. Chem. Soc.*, 127(2005) 13100.
4. L. Wang, L. Zhang, J. Zhang, *Electrochem. Commun.* 13 (2011) 447.
5. H.-S. Oh, J.-G. Oh, B. Roh, I. Hwang, H. Kim, *Electrochem. Commun.* 13 (2011) 879.
6. B. Lim, H. Kobayashi, T. Yu, J. Wang, M. J. Kim, Z.-Y. Li, M. Rycenga, Younan Xia, *J. Am. Chem. Soc.* 132 (2010) 2506.
7. M. S. El-Deab, T. Sotomura, T. Ohsaka, *Electrochim. Acta* 52 (2006) 1792.
8. Md. Rezwan Miah, T. Ohsaka, *Electrochim. Acta* 54 (2009) 5871.
9. S. S. Kumar, K.L.N. Phani, *J. Power Sources* 187 (2009) 19.
10. F. Terzi, C. Zanardi, S. Daolio, M. Fabrizio, R. Seeber, *Electrochim. Acta* 56 (2011) 3673.
11. A. Stoyanova , S. Ivanov, V. Tsakova , A. Bund, *Electrochim. Acta* 56 (2011) 3693.
12. Y. Zhang ,V.Suryanarayanan, I. Nakazawa, S. Yoshihara , T. Shirakashi, *Electrochim. Acta* 49 (2004) 5235.
13. S. Iijima, *Nature* 354(1991) 56.
14. M. Sathiya, A. S. Prakash, K. Ramesha, J−M. Tarascon, A. K. Shukla, *J. Am. Chem. Soc.*, 133(2011)16291.
15. S. Wang, F. Yang, S. P. Jiang, S. Chen, X.Wang, *Electrochem. Commun.* 12 (2010) 1646−1649

16. T. J. Davies, M.E. Hyde, R.G. Compton, *Angew. Chem. Int. Edit*. 44 (2005) 5121.
17. T. Welton, *Chem. Rev*. 99 (1999) 2071.
18. J.S. Wilkes, *J. Mol. Catal. A: Chemical* 214 (2004) 11
19. Y. Zhang, J. Zheng, *Electrochem. Commun*. 10 (2008) 1400.
20. K. Ding, G. Yang, *Electrochim. Acta* 55 (2010) 2319.
21. K. Ding, F. Cheng, *Synth. Met*. 159(2009) 2122.
22. K. Ding, M. Cao, *Russ. J. Electrochem*. 44(2008) 977.
23. M. Guerra-Balcázar , D. Morales-Acosta , F. Castaneda , J. Ledesma-García , L.G. Arriaga, *Electrochem. Commun*. 12 (2010) 864
24. V. Radmilovic, H. A. Gasteiger, P. N. Ross, *J. Catal*. 154(1995) 98.
25. M.-R. Yang, T.-H. Teng, S.-H. Wu, *J. Power Sources* 159(2006)307
26. C. Bao, M.Jin, R.Lu, T. Zhang, Y. Zhao, *Mater. Chem. Phys*. 82 (2003) 812.
27. G. Zhan, J. Huang, M. Du, I. Abdul-Rauf, Y. Ma, Q. Li, *Mater. Lett*. 65 (2011) 2989.
28. H. L. Ma ,W.J. Jin , L. Xi, Z. J. Dong, *Spectrochim. Acta Part* A 74 (2009) 502.
29. F. Shi, Y. Deng, *Spectrochim. Acta Part A* 62 (2005) 239.
30. Y. Ikezawa , T. Sawatari, H. Terashima, *Electrochim. Acta* 46 (2001) 1333.
31. D. Hulicova-Jurcakova , M. Seredych , G. Q. Lu , N.K.A.C. Kodiweera, P. E. Stallworth , S. Greenbaum , T. J. Bandosz, *Carbon* 47 (2009) 1576.
32. D.A. Bulushev, I. Yuranov, E. I. Suvorova, P. A. Buffat,L. Kiwi-Minsker, *J. Catal*. 224 (2004) 8.
33. C.E. Banks, A. Crossley, C. Salter, S.J. Wilkins, R.G. Compton, Carbon, *Angew. Chem. Int. Ed*. 45 (2006) 2533.
34. A.N. Shipway, M. Lahav, R. Gabai, I. Willner. *Langmuir,* 16 (2000) 8789.
35. D. Zhang, T. Okajima, F. Matsumoto, T. Ohsaka, *J. Electrochem. Soc*. 151(2004) D31.
36. M. Wang, Y.-J. Li, Z.-X. Xie, C. Liu, E.S. Yeung, *Mater. Chem. Phys*. 119 (2010)153
37. Y.-J. Li, W.-J. Huang, S.-G. Sun, *Angew. Chem. Int*. Ed. 45 (2006) 2537.
38. S. Yun, Y.-K. Park, S.K. Kim, S. Park, *Anal. Chem*. 79 (2007) 8584.
39. S. Sun, N. Jiang, D. Xia, *J. Phys. Chem*. C, 115(2011) 9511.
40. I. Danaee, M. Jafarian, A. Mirzapoor, F.Gobal, M. G. Mahjani, *Electrochim. Acta* 55(2010) 2093.
41. A. Kongkanand, S. Kuwabata, *Electrochem. Commun*. 5 (2003) 133.
42. M.S. El-Deab, T. Ohsaka, *Electrochem. Commun*. 4 (2000) 288.
43. K. Matsubara, K. Waki, *Electrochim. Acta* 55 (2010) 9166.
44. Z. Qia, H. Geng, X. Wang, C. Zhao, H. Ji, C. Zhang, J. Xu, Z. Zhang, *J. Power Sources* 196 (2011) 5823.
45. K. Ding, Z. Jia, Q.Wang, X. He, N.Tian, R. Tong, X.Wang, *J. Electroanal. Chem*. 513(2001)67.
46. K. Ding, G.Yang, S. Wei, P. Mavinakuli, Z. Guo, *Ind. Eng. Chem. Res*. 49(2010)11415.
47. H. Meng, P. K. Shen, *Electrochem. Commun*. 8 (2006) 588.
48. K. Shimizu, I. F. Cheng, C. M. Wai, *Electrochem. Commun*. 11 (2009) 691.
49. K. Ding, H. Jia, S. Wei, Z. Guo, *Ind. Eng. Chem. Res*. 50(2010)7077.